Physics of small metal clusters: Topology, magnetism, and electronic structure

B. K. Rao* and P. Jena
Physics Department, Virginia Commonwealth University, Richmond, Virginia 23284
(Received 4 March 1985)

The electronic structure of small clusters of lithium atoms has been calculated using the self-consistent-field, molecular-orbital method. The exchange interaction is treated at the unrestricted Hartree-Fock level whereas the correlation is treated perturbatively up to second order by including pair excitations. This is done in two steps, one involving only the valence electrons and the other including all the electrons. A configuration-interaction calculation has also been done with all possible pair excitations. The equilibrium geometries of both the neutral and ionized clusters have been obtained by starting from random configurations and using the Hellmann-Feynman forces to follow the path of steepest descent to a minimum of the energy surface. The clusters of Li atoms each containing one to five atoms are found to be planar. The equilibrium geometry of a cluster is found to be intimately related to its electronic structure. The preferred spin configuration of a cluster has been found by minimizing the total energy of the cluster with respect to various spin assignments. The planar clusters are found to be less magnetic than expected by Hund's-rule coupling. For three-dimensional clusters, however, the magnetism is governed by Hund's rule. The effect of correlation has been found to have decisive influence on the equilibrium topology and magnetism of the clusters. The binding energy per atom, the energy of dissociation, and the ionization potential of the clusters are compared with experiment and with previous calculations. The physical origin of the magic numbers and the effect of the basis functions on the calculated properties have also been investigated.

I. INTRODUCTION

One of the popular methods for studying the electronic structure and properties of metals and metal defects has been to represent the infinite system by a finite molecular cluster of constituent atoms.[1] While these calculations have yielded valuable information regarding the electronic structure of point defects, a nagging concern has always been to assess the sensitivity of the results to the finite size of the molecular clusters. This problem arises since a very large fraction of the atoms in small clusters lie on the surface. In addition, how fast the properties in the molecular clusters approach the bulk value may depend on the property being investigated.[2] This aspect of using molecular clusters as fragments of the bulk metal will be discussed in detail in a forthcoming paper.

In this paper we treat a different aspect of the physics of small metal clusters. Recent improvements in the matrix-isolation method and the development of molecular-beam technology have enabled researchers to produce small metal clusters consisting of two to a few hundred atoms per cluster. Studies of the structural, electronic, and magnetic properties of these clusters have revealed novel features. For example, recent experiments[3] on alkali-metal clusters have shown that clusters consisting of a certain number of atoms are more abundant than others. The number of atoms in the more abundant species is called the "magic number," the origin of which has been attributed to the electronic shell structure[3] of the clusters. The electronic structure of small clusters can also be used to understand how the localized electrons in an atom transform to delocalized (conduction) states in a metal. The change from the "bond picture" to the "band picture" is a topic of interest not only in physics but also in chemistry. The magnetism of small clusters is also a fascinating problem. While a metal may be nonmagnetic in the bulk phase, small clusters of its atoms may exhibit magnetism.[4] This can be studied through electron-spin-resonance (ESR) techniques. Despite considerable theoretical and experimental works in this field, answers to some basic questions are lacking. For example, what mechanism determines the spin configuration of a small cluster? Does the magnetic behavior of a cluster have any relationship to its topology? What is the equilibrium geometry of a cluster and is it determined solely by its electronic structure? What is the origin of the magic numbers? Are the magic numbers determined by the electronic shell structure as the recent jellium calculations[3] seem to suggest or are there more subtle effects? In this paper we address these issues.

Many of these questions cannot be answered directly from experiments. Both theory and experiment are necessary to understand the link between the equilibrium geometry, electronic structure, and magnetism. Theoretically, one can obtain the optimized geometry of a cluster by minimizing the total energy with respect to all variable parameters, e.g., bond lenths, bond angles, and spin configurations. The binding energy per atom, the dissociation energy of the molecule, the ionization potential (energy to remove one electron from the molecule), and the electron spin density at the atomic sites in the cluster can be compared with the experimental results. Once a consistent agreement is achieved between the available experimental data and theory, one can regard the optimized

geometry of the cluster obtained theoretically to be the "true" topology of the cluster.

This may be much more difficult than it appears since the theoretical results may depend upon various approximations, e.g., the level of exchange approximation (Hartree-Fock versus local density), treatment of correlation, and the limitations of the basis functions used. For small clusters consisting of only a few atoms, it is possible to carry out sophisticated calculations including the exchange interaction at the Hartree-Fock level and the correlation contribution using configuration interaction. Clearly, these calculations are prohibitively difficult for larger clusters of light atoms as well as for small clusters of transition-metal atoms. For these systems, one is then forced to use less sophisticated methods such as those based on the pseudopotential scheme and local-density approximation.[5] On the numerical side, most of the cluster calculations use molecular orbitals as a linear combination of atomic orbitals (LCAO). The atomic orbitals are either taken as numerical wave functions (as is done in the discrete variational method[1]) or are expanded in terms of a set of Gaussian orbitals.[6] The advantage of the latter approach is that the integrals can be carried out analytically, thus enabling an accurate determination of the total energy. The difficulty, however, is in confirming that the results are insensitive to the choice of the number of Gaussian functions used to fit the atomic orbitals. While the discrete variational method is not plagued by this problem, the evaluation of the total energy is difficult since one has to resort to numerical integration to obtain the matrix elements. One then needs to know how sensitive the total-energy calculations are to the choice of integration points.

Despite the difficulties cited above, numerous studies have been done on small clusters[5,7–11] using different approximations for exchange and correlation and different choices of basis sets. It is customary to compare one's result with other existing calculations. While such comparisons can give qualitative ideas of the validity of one approximation versus another, no quantitative information can be extracted since the results may also depend on numerical details in the calculations.

In this paper we present a thorough investigation of the electronic structure of small clusters of lithium atoms as an example. For these clusters, consisting of up to five atoms, we have calculated the total energy and topological parameters of the optimized geometry within the unrestricted Hartree-Fock (UHF) approximation. These calculations were repeated by including the correlation contribution at three different levels. The first two schemes take into account correlation effects perturbatively by including pair excitations of valence electrons and all electrons separately. We have also performed calculations using configuration interactions with all possible pair excitations. The comparisons of these results reveal the effect of correlation at various levels of approximation on the equilibrium geometry and binding energy. This comparison does not suffer from the ambiguity that arises due to basis-set choice since all calculations have been done with the same basis. The magnetism of the clusters was investigated by minimizing the energy of the optimized clusters with respect to their spin configurations. The clusters with planar structures were less magnetic than expected from Hund's-rule coupling. However, for three-dimensional clusters, the magnetism was dictated by Hund's rule. We should clarify at this point what is meant by Hund's-rule coupling in real clusters. Hund's rule, which states that maximizing spins always lowers the total energy, was empirically derived from atomic spectra. Consequently, it should apply to situations with spherical symmetry. Real clusters, especially when they are small, are not spherical. Therefore, the applications of Hund's-rule coupling in the understanding of spin states of small clusters may not be meaningful. In this paper, we refer to Hund's rule as it applies to results of spherical jellium clusters and its relationship to real clusters.[4] We find that electronic structure, equilibrium geometry, and magnetism are found to be closely linked.

We have also calculated the ionization potential and energy of dissociation for all the clusters. The results are compared with experiments as well as with available theories. In Sec. II we present a brief description of the theory used. Section III discusses our results for Li clusters. A summary of our results and conclusions is given in Sec. IV.

II. THEORETICAL METHODS

For the calculation of the energy of the clusters, we have used a self-consistent-field (SCF), molecular-orbital (MO) method. In this approach one starts with an assumed geometry of the cluster as a molecule. The total wave function describing the system is a Slater determinant formed out of molecular spin orbitals. For the UHF procedure, in general, the number of electrons with spin up (denoted by α) and those with spin down (denoted by β) are not the same. In such a case the electronic energy is given by

$$E=\sum_{i=1}^{p+q} H_{ii}+\frac{1}{2}\left[\sum_{i=1}^{p+q}\sum_{j=1}^{p+q} J_{ij}-\sum_{i=1}^{p}\sum_{j=1}^{p} k_{ij}^{\alpha}-\sum_{i=1}^{q}\sum_{j=1}^{q} k_{ij}^{\beta}\right], \tag{1}$$

where p and q denote the number of α and β electrons, respectively. H_{ii} represents the one-electron part of the matrix elements. The Coulomb and exchange integrals are defined as

$$J_{ij}=\int\int \psi_i^*(1)\psi_j^*(2)\left[\frac{1}{r_{12}}\right]\psi_i(1)\psi_j(2)d\tau_1 d\tau_2 \tag{2}$$

and

$$k_{ij}^{\alpha}=\int\int \psi_i^{\alpha}(1)\psi_j^{\alpha}(2)\left[\frac{1}{r_{12}}\right]\psi_j^{\alpha}(1)\psi_i^{\alpha}(2)d\tau_1 d\tau_2 , \tag{3}$$

where ψ_i^{α} denotes a moelcular orbital with spin α. One can express the MO as a linear combination of atomic orbitals ϕ,

$$\psi_i^{\alpha\,(\beta)}=\sum_{\mu} C_{\mu i}^{\alpha\,(\beta)}\phi_{\mu} . \tag{4}$$

The combination coefficients C define the density matrices

$$P^{\alpha}_{\mu\nu}=\sum_{i=1}^{p} C^{\alpha}_{\mu i}C^{\alpha}_{\nu i}$$

and

$$P^{\beta}_{\mu\nu}=\sum_{i=1}^{q} C^{\beta}_{\mu i}C^{\beta}_{\nu i}\ . \tag{5}$$

The sum of both the density matrices is given by $P_{\mu\nu}$. Then the energy of Eq. (1) is rewritten in the LCAO approximation as

$$E=\sum_{\mu,\nu} P_{\mu\nu}H_{\mu\nu} + \frac{1}{2}\sum_{\mu,\nu,\lambda,\sigma}(P_{\mu\nu}P_{\lambda\sigma}-P^{\alpha}_{\mu\lambda}P^{\alpha}_{\nu\sigma}-P^{\beta}_{\mu\lambda}P^{\beta}_{\nu\sigma})(\mu\nu\,|\,\lambda\sigma)\ , \tag{6}$$

where

$$(\mu\nu\,|\,\lambda\sigma)=\int\int \phi_{\mu}(1)\phi_{\nu}(1)\left[\frac{1}{r_{12}}\right]\phi_{\lambda}(2)\phi_{\sigma}(2)d\tau_1 d\tau_2\ . \tag{7}$$

The next step is to find optimum values of the coefficients $C^{\alpha}_{\mu i}$ and $C^{\beta}_{\mu i}$ by carrying out variations of the α and β orbitals independently. One then obtains two sets of coupled equations:

$$\sum_{\nu}(F^{\alpha}_{\mu\nu}-\epsilon^{\alpha}_{i}S_{\mu\nu})C^{\alpha}_{\nu i}=0$$

and

$$\sum_{\nu}(F^{\beta}_{\mu\nu}-\epsilon^{\beta}_{i}S_{\mu\nu})C^{\beta}_{\nu i}=0\ , \tag{8}$$

where $S_{\mu\nu}$ and $F_{\mu\nu}$ are the overlap and Fock matrices, respectively, and ϵ_i are the one-electron energies. $F_{\mu\nu}$ is defined by

$$F^{\alpha(\beta)}_{\mu\nu}=H_{\mu\nu}+\sum_{\lambda,\sigma}[P_{\lambda\sigma}(\mu\nu\,|\,\lambda\sigma)-P^{\alpha(\beta)}_{\lambda\sigma}(\mu\lambda\,|\,\nu\sigma)]\ . \tag{9}$$

This generalization of Roothaan's equations was first given by Pople and Nesbet.[12] Starting with a set of trial density matrices P^{α} and P^{β}, one obtains solutions to Eq. (8) by an iterative procedure that can be continued until self-consistency is reached.

In the LCAO procedure of Eq. (4), one can use atomic orbitals in any form. For our work we have chosen to use a Gaussian representation for the atomic orbitals. In this, one expresses the atomic orbitals as a sum of Gaussian-type orbitals.[6,13–15] We write

$$\phi_{\mu}(\mathbf{r})=\sum_{k} d_{\mu k}g_{\mu}(\alpha_{\mu k},\mathbf{r})\ , \tag{10}$$

where $d_{\mu k}$ are the combination coefficients and g_{μ} are the Gaussian-type orbitals. For different symmetries these are given by

$$g_{\mu}=\exp(-\alpha_{\mu k}r^2) \tag{11}$$

for s-type orbitals, and

$$g_{\mu x}=x\exp(-\alpha_{\mu k}r^2) \tag{12}$$

for the components of p-type orbitals. Among the Gaussian-type basis sets developed for efficient application of Hartree-Fock MO theory, the simplest are the minimal Slater-type basis sets, least-squares fitted by N Gaussian as given in Eq. (10) (STO-NG).[6] The next level of sophistication is the split-valence basis[14,15] of s and p functions where two ϕ_{μ}'s are used for each valence orbital. In this case each ϕ_{μ} is obtained by separate contraction of a different set of primitive Gaussians. This is expected to introduce sufficient flexibility in the basis sets so that the interactions in a molecule are reproduced reasonably well. Some examples of these are the 4-31G, 5-31G, and 6-31G basis sets.[6,14] In all these basis sets one would normally expect the lithium atoms to be represented by one $1s$ and one $2s$ function for the MO's. But for the valence shell, p-like orbitals are also added to the basis sets. This facilitates the simulation of various types of excitations in terms of which interatomic interactions can be expressed. In the least-squares-fitting process the exponents $\alpha_{\mu k}$ and coefficients $d_{\mu k}$ are obtained for a specific value of k. But the values of $\alpha_{\mu k}$ need to be changed slightly from their atomic values to represent the molecules better. Therefore, one usually uses a scale factor s such that

$$\alpha_{\mu k}(\text{molecular})=s^2\alpha_{\mu k}(\text{atomic})\ . \tag{13}$$

This scale factor is obtained by calculating certain properties of several molecules involving this atom and other atoms and choosing a suitable value for s which would simulate these properties as closely as possible. Thus, there is no unique value for s. In addition to this, more ambiguity can also enter an LCAO calculation using Gaussian basis sets through the choice of k, the number of Gaussians being contracted at a time. By making k very large one expects to minimize the errors caused by the fitting procedure. Another possible improvement is to use a large number of MO's in the SCF procedure so that the electrons can delocalize freely and can mimic the interactions as accurately as possible. However, in adding extra MO's one has to be careful about the basis-set superposition error.[16]

With so many possibilities of choosing different atomic basis sets one would have to justify the choice of one particular basis. The most important reason for choosing a particular basis would be governed by the size limitations in the computer. With this in view, one has to choose a limited basis set which should represent the properties suitably. Comparison of results from various types of limited basis sets has been made in our work and is discussed in the next section.

To improve the results of the UHF procedure one must include the effect of correlation. In the present work it is done by an approach suggested by Møller and Plesset[17] (MP) and developed by Binkley and Pople[18] for SCF LCAO-MO procedure. For this, one writes the correct Hamiltonian in the form

$$H=\sum_{p}\tilde{F}_p+\left[H-\sum_{p}\tilde{F}_p\right]\ , \tag{14}$$

where $\tilde{F}_p$ is the one-electron Hartree-Fock Hamiltonian which has the UHF orbitals as eigenfunctions. The summation is over all electrons. The terms within large parentheses in Eq. (14) are then treated as a perturbation

and correlation due to this perturbation is calculated up to several orders using Rayleigh-Schrödinger perturbation theory. In this case, the energy correct to first order is the Hartree-Fock energy, $E_{\rm UHF}$. The second-order energy is given by

$$E_2 = -\sum_{\substack{i,j \\ (i<j)}}^{\rm occ} \sum_{\substack{a,b \\ (a<b)}}^{\rm unocc} \frac{|\langle ij|r^{-1}|ab-ba\rangle|^2}{(\epsilon_a+\epsilon_b-\epsilon_i-\epsilon_j)} , \quad (15)$$

where

$$\langle ij|r^{-1}|ab\rangle = \int\int \psi_i^*(1)\psi_j^*(2)\left[\frac{1}{r_{12}}\right]\psi_a(1) \times \psi_b(2)d\tau_1 d\tau_2 . \quad (16)$$

In Eq. (15) ψ_i and ψ_j are occupied and ψ_a and ψ_b are unoccupied. The unoccupied orbitals are sometimes denoted as virtual orbitals. Thus, after obtaining the UHF energy, we can make corrections due to correlation using this approach. In the present work the perturbation expansion is done up to second order only (MP2) and the total energy is given as

$$E_{\rm MP2} = E_{\rm UHF} + E_2 . \quad (17)$$

This procedure for the calculation of $E_{\rm MP2}$ can be done for all the electrons in the system (AEMP2). However, we have also tried to include the excitations of the valence electrons only (VEMP2). As will be apparent from later sections, in most cases the VEMP2 calculation represents most of the correlation. This "frozen-core" approximation works reasonably well because the correlation energy associated with the core electrons varies little with the environment.

In addition to this, we have also used the configuration-interaction (CI) procedure including all pair excitations and have calculated the correlated energy nonperturbatively. The comparison of all the results is given in the next section.

All the above procedures are for obtaining the energy of a cluster in a given geometry. For finding the best geometry of a cluster (which would give the lowest energy) there are several available procedures. For our calculations here, we start with a random geometry, calculate the Hellmann-Feynman forces at the atoms, and follow the path of steepest descent to a minimum of energy. For all the results presented in this paper, the root-mean-square Hellmann-Feynman force at any nuclear site was considered to be zero if its magnitude was found to be less than 0.0003 hartrees/bohr. After the UHF calculations we start with the equilibrium geometry obtained from these calculations and study the variations of the energy with minor changes in the topological parameters. The energies thus computed at points in the vicinity of the initial values define a multidimensional energy surface. This surface is fitted to a function from which the new equilibrium geometry (including correlations) is obtained by finding the new energy minimum. The above two processes are repeated successively until the root-mean-square force falls below 0.0003 hartrees/bohr.

III. RESULTS FOR Li CLUSTERS

In this section we discuss the results for clusters of lithium atoms. We have chosen this example for several reasons. Of all metals, lithium has the smallest atom. Since the number of electrons (core and valence) is small, it is computationally feasible to study the various aspects of theory pointed out earlier. In addition, there is a great wealth of experimental data with which our results can be compared.

We have investigated the dependence of our results on the choice of basis sets and the level of approximation for correlation. For Li clusters consisting of up to five atoms, we have obtained the total ground-state energies, equilibrium geometries, spin configurations, ionization potentials, and dissociation energies. For the sake of clarity we discuss these aspects separately.

A. Choice of basis sets

As mentioned in the preceding section, in the molecular-orbital representation the wave functions are represented by a linear combination of atomic orbitals. The atomic-orbital wave functions are, in turn, given in terms of a combination of Gaussian functions. As an illustration, we have used five different Gaussian basis sets: the minimal Slater-type orbital, fitted by three Gaussians (STO-3G),[6] the improved STO-6G,[13] the split-valence 6-31G,[14,19] the Dunning basis,[20] and the modified Dunning basis.[21] In each case the contractions of the primitive Gaussians are shown in Table I. The latter two basis sets were chosen because they provide atomic properties in excellent agreement with experiment. Using these basis sets, we have calculated the total energy and ionization potential of the Li atom and the total energy, equilibrium bond length, and binding energy of the Li_2 molecule. The results are presented in Table I. Several remarks are in order. There is no unique rule for choosing the best basis set. A particular basis set, for example, may give the best result for atomic properties while it may be completely inadequate to describe molecular properties. This is what is quite noticeable in Table I. Note that the modified Dunning basis yields the best energy and ionization potential for the atom. However, it yields much poorer agreement with experiment for bond length and binding energy of Li_2 than that obtained from the use of STO-6G basis. The reasons are clear. To obtain the best energy of the atom, one needs to improve the core states considerably. However, in forming a molecule, the deeply bound core electrons do not play too significant a role. Here the valence electrons are important. This is not to imply that an inadequate representation of the core states in comparison to valence orbitals would yield satisfactory results for the binding energy of the molecule. As valence electrons are allowed to relax, the core-electron orbitals get influenced because of antishielding. Thus, a compromise has to be reached between the proper representation of valence- and core-electron states. From the results of Table I, we see that the STO-6G basis yields the best binding and bond length of Li_2 when compared to experiment. Therefore, for all the remaining calculations in Li clusters, we have used the STO-6G basis. It is, of course, al-

TABLE I. Comparison of results obtained from different basis sets. Total energies are given for Li, Li^+ ion, and Li_2 molecule. The ionization potential E_{IP}, binding energy E_B, and interatomic distance for Li_2 at equilibrium (a) are also presented. In the basis set notation the left-hand side denotes the primitive Gaussians and the right-hand side is the final set of contracted Gaussians.

Basis details	Calculation details	E_{Li} (a.u.)	E_{Li^+} (a.u.)	E_{IP} (eV)	E_{Li_2} (a.u.)	a (Å)	E_B (eV)
6-31G	HF	−7.431 236	−7.235 480	5.235	−14.866 317	2.815	0.105
(10*s*4*p* /3*s*2*p*)	AEMP2	−7.431 520	−7.235 658	5.327	−14.882 560	2.810	0.531
	CI	−7.431 553	−7.235 643	5.329	−14.893 434	2.760	0.825
STO-6G	HF	−7.399 931	−7.221 333	4.858	−14.808 879	2.699	0.245
(12*s*6*p* /2*s* 1*p*)	AEMP2	−7.400 186	−7.221 578	4.858	−14.825 713	2.678	0.689
	CI	−7.400 238	−7.221 557	4.860	−14.837 075	2.646	0.995
Dunning basis	HF	−7.432 392	−7.236 210	5.336	−14.861 293	2.858	−0.095
(10*s* /4*s*)	AEMP2	−7.443 066	−7.247 030	5.332	−14.890 026	2.911	0.106
	CI	−7.445 272	−7.249 317	5.330	−14.901 531	2.983	0.299
Modified Dunning	HF	−7.432 392	−7.236 210	5.336	−14.870 469	2.783	0.155
basis (10*s*2*p* /4*s* 1*p*)	AEMP2	−7.443 229	−7.247 066	5.336	−14.906 616	2.760	0.548
	CI	−7.445 465	−7.249 343	5.335	−14.918 652	2.699	0.754
STO-3G	HF	−7.315 526	−7.135 448	4.898	−14.638 747	2.699	0.209
(6*s*3*p* /2*s* 1*p*)	AEMP2	−7.315 782	−7.135 674	4.899	−14.655 495	2.694	0.651
	CI	−7.315 836	−7.135 653	4.900	−14.666 734	2.630	0.954
Experiment				5.392[a]		2.672[a]	1.03[a]

[a]Reference 30.

ways possible to use more extensive basis sets[22] than what is used here. However, in doing so, the self-consistent calculations for the clusters as done here would become prohibitively difficult. Thus, a compromise has to be made between the accuracy desired in the calculations and the size of basis sets which influence computer time.

B. Level of correlation approximation

In the present work we have obtained results for all the basis sets using UHF, AEMP2, and CI methods. In Table I we compare the total energies and ionization potentials of the Li atom and the total energy, bond length, and binding energy of the Li_2 molecule. The inclusion of correlation (at the AEMP2 or CI level) lowers each of the energies as expected. For a given basis set, note that the improvements in the ionization potential of the atom are only minimal when the two levels of correlation are considered. However, the CI result for the binding energy of the Li_2 molecule is significantly better than the corresponding perturbative AEMP2 result. The bond length, on the other hand, is not very sensitive to the level of correlation approximation.

Another interesting observation can be made from Table I. We note that the binding energies of the Li_2 molecule in the CI calculations using different basis sets differ by as much as 0.7 eV (see the STO-6G and Dunning basis). This is of the same order as the difference between the Hartree-Fock and the CI results of a given basis set. Thus, we wish to emphasize that in situations where two different calculations (e.g., local density versus CI, pseudopotential versus all-electron calculations) yield nearly equal results, caution should be exercised in justifying the approximations involved unless both the calculations utilize identical numerical procedure.

From further investigation of the effect of various levels of correlation on the electronic and structural properties of clusters, we list in Table II the total energy and bond lengths of neutral Li clusters consisting of up to five atoms using the STO-6G basis set. The optimized geometries for all the cases are given schematically in Fig. 1. All the forms shown are planar in structure. Correlation contributions have been calculated at three different levels, i.e., VEMP2, AEMP2, and CI. As before, the total energy of each cluster is lowered with increasing improvements in correlation approximation. The differences in topological parameters between Hartree-Fock and various levels of correlation approximations are not very large. The clusters tend to be more closely packed as correlation is included. We wish to emphasize here, again, that for each of the calculations presented in Table II the geometries were optimized starting initially from random structures. Since the numerical details for all these clusters are identical, the results in Table II represent the *true* influence of correlation on the topological parameters and total energies. It is quite clear that even within the Hartree-Fock scheme, one can obtain the right equilibrium geometry for a cluster. The bond lengths are also in reasonable agreement with the CI results. However, we will show later in this paper that while the structure of a cluster can be well described by the Hartree-Fock scheme, many of the electronic properties require the inclusion of

TABLE II. Total energy and bond lengths (a,b,c,d) of neutral lithium clusters at the corresponding optimal geometries. The shape of the geometries are given in Fig. 1. Energies and bond lengths are given in atomic hartrees and angstroms, respectively. The spin configuration for which the energy is the lowest is shown in the second column for each cluster.

N	Quantity	HF	VEMP2	AEMP2	CI
1	$E(\uparrow)$	−7.399 931	−7.399 931	−7.400 186	−7.400 238
2	$E(\uparrow\downarrow)$	−14.808 879	−14.824 828	−14.825 713	−14.837 075
	a	2.699	2.696	2.678	2.646
3	$E(\uparrow\downarrow\uparrow)$	−22.231 568	−22.241 549	−22.243 038	−22.253 448
	a	2.698	2.695	2.687	2.684
	b	3.045	3.175	3.162	3.266
4	$E(\uparrow\downarrow\uparrow\downarrow)$	−29.650 737	−29.686 364	−29.688 658	−29.708 516
	a	3.033	3.002	2.997	2.938
	b	2.524	2.576	2.570	2.612
5	$E(\uparrow\downarrow\uparrow\downarrow\uparrow)$	−37.093 920	−37.113 595	−37.116 357	−37.137 382
	a	2.904	2.920	2.928	2.880
	b	3.520	2.963	2.923	2.991
	c	2.911	2.980	2.979	2.939
	d	2.903	2.929	2.919	2.934

correlation effects for proper understanding. The spin configurations for clusters in Table II are given in the second column. These correspond to the lowest-energy states as compared to other possible spin configurations. We will discuss this aspect more fully in the later sections. In what follows, we shall only present results obtained from complete CI calculations.

C. Electronic structure

We now discuss the role of electronic structure on magic numbers and equilibrium geometries of clusters. Recently, Knight *et al.*[3] have observed conspicuously large peaks in the mass spectra of Na clusters. These peaks occurred for $N=2$, 8, 20, 40, 58, and 92 where N is the number of atoms in the cluster. Similar peaks have been observed by other workers earlier for Na,[23] Li,[24] and rare-gas-atom clusters.[25] Knight *et al.*[3] explained the occurrence of these "magic numbers" in terms of an electronic shell model. Using a jellium model for clusters, they showed that the energy per atom in a cluster is lowered in comparison to its adjacent clusters when the electron shells are completely filled. This simple explanation and its remarkable ability to explain the experimental features imply that the abundance of clusters is governed by a very fundamental principle. In the following discussion we shall show that such an optimism is premature, at least for small clusters, and that the abundances of clusters are governed by many different competing mechanisms. Moreover, kinetic effects[16] also have to be considered while dealing with these magic numbers.

In Fig. 2 we present the total energy per atom of Li clusters consisting of $N=1$ to 42 atoms per cluster obtained from a spin-polarized density-functional jellium calculation. In the jellium model, the positive charges are

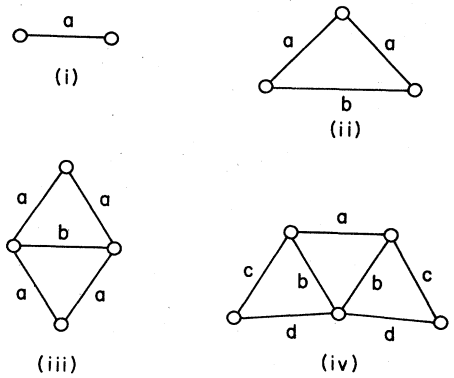

FIG. 1. Shape of optimum geometries of Li_N clusters up to $N=5$.

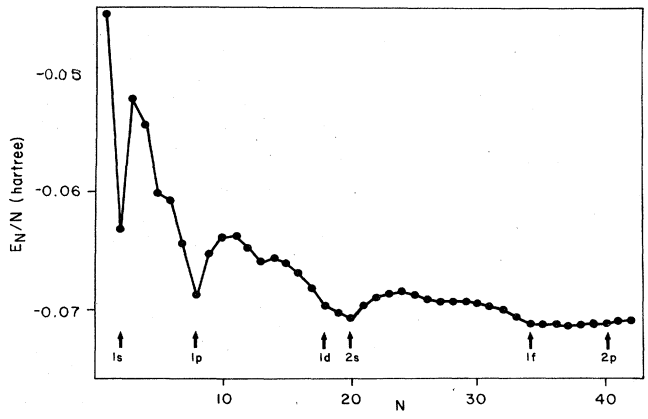

FIG. 2. Plot of energy per atom versus N obtained from jellium calculations. The shell filling has been indicated by suitable labels at the bottom of the graph.

modeled by a sphere of homogeneous density n_0, namely,

$$n_{\text{ext}}(\mathbf{r})=n_0\Theta(\mathbf{R}-\mathbf{r}) , \tag{18}$$

where R is the radius of the sphere and is related to the number N of atoms in the cluster through the relation

$$R=r_s N^{1/3} . \tag{19}$$

The electron density parameter r_s is given by

$$\frac{1}{n_0}=\frac{4\pi}{3}r_s^3 .$$

We have used the bulk value of r_s for all the jellium calculations of Li clusters. The electronic structure of these spherical jellium clusters is obtained self-consistently by solving the density-functional equation.[27] Before we discuss the results in Fig. 2 we want to remind the reader that the jellium model for small clusters is an oversimplification of reality. As pointed out earlier, clusters of up to five Li atoms do not even form a three-dimensional structure. This aspect will have strong influence on magnetism as will be discussed later.

In Fig. 2 we see distinct dips in the energy per atom for clusters with $N=2$, 8, 20, 34, and 40. Thus, on energy grounds, one would conclude, for example, that an $N=2$ cluster is more likely to form than either an $N=1$ or $N=3$ cluster. This would make $N=2$ a magic number. Clusters containing $N=2$, 8, 20, 34, and 40 electrons correspond to situations where $1s$, $1s1p$, $1s1p1d2s$, $1s1p1d2s1f$, and $1s1p1d2s1f2p$ orbitals are filled. These results agree with the jellium calculations of Knight *et al.*[3] and have the same features as experimental results in Na. In addition, we also see dips in the energy diagram for $N=5$, 13, 27, and 37. These correspond to half-filling of $1p$, $1d$, $1f$, and $2p$ orbitals, respectively. These features (which can be seen more pronouncedly in the second derivative of the energy plot[28]) are absent in the calculations of Knight *et al.* since theirs was a nonpolarized calculation whereas ours is spin polarized. In all our jellium calculations we found that maximizing the spin according to Hund's rule coupling always lowers the energy. Thus the $N=5$ cluster in the jellium model is a quartet, whereas it was a doublet in our calculations of the real cluster. In addition to this discrepancy, the jellium model also fails to explain other systematics in the mass spectra. For example, Knight *et al.* observed that the $N=14$ cluster is more abundant then either the $N=13$ or $N=15$ cluster. Our spin-polarized jellium cluster calculation would suggest just the opposite. Here we find the $N=13$ cluster to be more abundant than the $N=14$ cluster. Thus, the jellium model not only yields the wrong spin configuration but also fails to account for all the conspicuous peaks in the mass spectra.

The origin of the magic numbers, therefore, has to be looked for elsewhere. Here it is important to realize how the experimental information is obtained. In a typical experiment, one starts with the vapor (consisting of single atoms) which, upon cooling in a rare-gas-atom environment, condenses to form molecular clusters of different sizes. These clusters are then ionized and subsequently studied in a mass spectrometer. Thus, the magic numbers, seen in terms of conspicuously large peaks in the mass spectra, can be influenced at several different stages. First, it must be energetically favorable for a certain cluster to form more easily than its immediate neighboring sizes. Second, having formed, the cluster should have a high threshold against dissociation. Third, it must be easy to ionize this cluster. All these three effects may not always act in the same direction. Thus, one needs a complete understanding of the energy per atom, dissociation energy, and ionization potential of the clusters to understand the occurrence of magic numbers. It may also be necessary to consider kinetic effects[26] which may affect the cluster formation.

It is prohibitively difficult, with the present status of computer technology, to perform completely *ab initio* CI calculations of the energetics of Li clusters of up to 40 atoms per cluster and to determine their equilibrium topology. We, therefore, restrict our discussion concerning the magic numbers for Li to $N=5$. In Table III we list the total energy of the ionized clusters along with the topological parameters for their optimized geometry, energy per atom, the energy of dissociation, and the adiabatic ionization potential. These results are based on an STO-

TABLE III. Some properties of singly ionized clusters (total energy E_N^+ and optimized geometries) and neutral clusters [energy per atom, dissociation energy (ΔE), and ionization potential E_{IP}]. The geometries correspond to Fig. 1 and the bond lengths are given in angstroms. E_N^+ and E_N/N are given in hartrees. ΔE and E_{IP} are in eV.

	Ionized clusters		Neutral clusters		
N	E_N^+	Geometry	E_N/N	$E_{\text{IP}}=E_N^+-E_N$	$\Delta E=E_{N-1}+E_1-E_N$
1	−7.221 557		−7.400 238	4.860	
2	−14.677 998	$a=3.028$	−7.418 538	4.327	0.995
3	−22.140 043	$a=2.994$	−7.417 816	3.085	0.439
		$b=2.996$			
4	−29.569 373	$a=3.092$	−7.427 129	3.785	1.491
		$b=2.774$			
5	−37.025 352	$a=5.441$	−7.427 476	3.047	0.779
		$b=3.087$			
		$c=2.830$			
		$d=3.099$			

6G basis with full CI calculation. We have defined the dissociation energy as

$$\Delta E = -E_N + (E_{N-1} + E_1) , \tag{20}$$

where E_N is the total energy of the N-atom cluster and E_1 is the energy of a single atom. Thus a positive value of ΔE for an N-atomic cluster implies that it is stable against dissociation to an $N-1$ cluster and a free atom.

To facilitate the discussion of magic numbers, we plot in Fig. 3 the energy per atom, dissociation energy, and ionization potential of Li clusters. Note that the energy per atom for the $N=2$ cluster is lower than that for the $N=1$ or $N=3$ cluster, thus making the formation of $N=2$ clusters more likely than that of a $N=3$ cluster. The dissociation energy, on the other hand, for the $N=3$ cluster is lower than for the $N=2$ cluster. This implies that it is easier for a Li_3 cluster to dissociate to Li_2+Li than it is for a Li_2 molecule to dissociate to two Li atoms. However, the dissociation energy for the Li_3 cluster is about 0.5 eV and thus it is quite stable against dissociation. On the other hand, it is energetically more favorable for a Li_3 cluster to accept an additional Li atom to transform to a Li_4 cluster. It is probably for this reason that the abundance of Li_2 clusters is higher than that of Li_3 clusters. The ionization potential for the Li_3 cluster is much lower than that of the Li_2 cluster. Consequently, it is much easier to ionize Li_3 than the Li_2 cluster. Thus, the observed abundances have to be influenced by not only the formation of clusters but also by the ease with which they can be ionized. While the ionization potential arguments would make $N=3$ a magic number, the energy per atom and the dissociation energy arguments would make $N=2$ a magic number. Thus, the experimental observation of $N=2$ as a magic number leads to the conclusion that the higher energy per atom of $N=3$ and its easier transformation to a $N=4$ cluster make the abundance of Li_3 less likely than that of Li_2. The higher magic numbers have to be understood in a similar way. Unfortunately, it is difficult to carry out calculations of the type described here for larger clusters. We feel that the jellium model provides an incomplete picture of the occurrence of magic numbers and its apparent early success shrouds some interesting physics. In Fig. 3 we have also plotted the energy per atom, ionization potential, and dissociation energies for $N=1-$ to $N=5-$atom clusters by optimizing the geometries within the unrestricted Hartree-Fock scheme. Note that the UHF calculations fail to produce the systematics found in the complete CI calculations. We can therefore conclude that, although the geometries and bond lengths of clusters can be reasonably calculated in the UHF procedure, it fails to describe the electronic properties well. In Table IV we compare our results with previous CI calculations and available experimental results. We would like to remind the reader that in previous CI calculations (except for Li_2) the geometries have not been completely optimized. Thus, the discrepancy between our CI results and others could partly stem from the different geometries used. Some of the discrepancies can also originate from the details in the numerical procedure as discussed earlier. Despite this, the agreement between the various calculations and experiment is very reasonable.

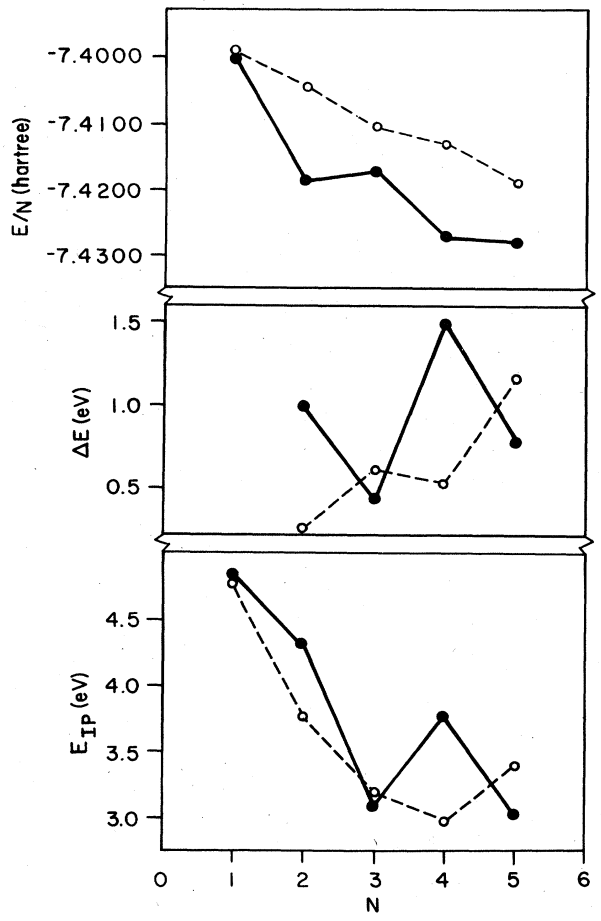

FIG. 3. UHF (dashed line) and CI (solid line) results for energy per atom, dissociation energy, and ionization potential.

We now discuss the relationship between the electronic structure and equilibrium geometry of the clusters. In Fig 4 we plot the charge density contours for $N=2$ to $N=5$ Li clusters. The presence of delocalized electrons can be clearly seen from these contour plots. In all these plots the charge density in the interatomic region is reasonably large because of these delocalized electrons. An understanding of the orbital character of these electrons is very useful in relating the electronic structure of clusters to their equilibrium geometries and magnetic configurations. In atomic calculations, the orbitals are characterized by angular momentum (l) and azimuthal quantum numbers (m). In real molecular clusters, on the other hand, such characterization is not possible. As mentioned earlier, an attempt to explain the magic numbers was made in terms of successive filling of angular momentum states in spherical jellium clusters. A comparable understanding can also be achieved for the molecular orbitals. For example, in the present case, we start with only $1s$ and $2s$ atomic orbitals and form a series of σ and σ^* molecular orbitals for the occupied stats. The σ^* orbitals are antisymmetric and therefore will have nodal planes. Comparing these with the p levels of the jellium model, one can say that the

TABLE IV. Comparison of results with previous CI calculations and available experimental values. The geometries correspond to Fig. 1. The units are as mentioned in the preceding tables. Note that in other CI calculations ($N \geq 3$) the geometries are not completely optimized.

N	Quantity	Present results	Other CI results	Experiment
2	a	2.646	2.694[a]	2.672[b]
	E_B	0.995	0.99[a]	1.03[b]
	E_{IP}	4.327		4.86±0.1[e]
3	a	2.684	2.815[c], 2.964[d]	
	b	3.266	3.329[c], 3.442[d]	
	E_B	1.434	1.49[c]	1.79[e]
	E_{IP}	3.085	4.0[c]	4.35±0.2[e]
4	a	2.938	3.080[f]	
	b	2.612	2.749[f]	
	E_B	2.925	2.263[f]	3.34±0.1[g]
	E_{IP}	3.785	4.54[f]	4.69±0.3[g]
5	a	2.880		
	b	2.991		
	c	2.939		
	d	2.934		
	E_B	3.704	2.774[h]	
	E_{IP}	3.047		

[a]Reference 31.
[b]Reference 30.
[c]Reference 9.
[d]Reference 10.
[e]Reference 32.
[f]Reference 11.
[g]Reference 33.
[h]Reference 8.

σ^* orbitals are p-like in character. Depending upon the position of the nodal planes, these can be described as p_x-, p_y-, or p_z-like in behavior. Proceeding with the MO picture, one would then expect these orbitals to be filled successively. Thus, for example, the outermost electrons of the Li_4 cluster will fill the s-like and the p_x-like (the choice of x, y, or z depends upon the choice of the axes) molecular orbitals, making the Li_4 ground state a spin singlet. Upon forcing the configuration to go to the next higher state, p_x- and p_y-like orbitals would be filled. This would permit Hund's rule to force the state to be a spin triplet. In either case, the atoms would lie in the x-y plane, making the cluster a planar one. However, for clusters of $N \geq 7$, the p_z-like states will start filling up and the clusters will become three dimensional. This is in complete agreement with the observation of Martins *et al.*[5] To confirm the link between the filling of the molecular orbitals and dimensionality of clusters further, we have performed self-consistent calculations of the Be_4 cluster.[29] Here, there are eight valence electrons, and thus p_z-like orbitals would be filled and the optimized geometry will be expected to be nonplanar. Indeed, the equilibrium structure was found to be three dimensional.

In the present calculations, for Li clusters, we had included $2p$ functions in the atomic basis to introduce flexibility and to simulate the interactions of the valence electrons properly. This also helps to demonstrate the relation of the topology and the electronic structure in terms of the successive filling of the electronic states. In Table V we present the orbital charges connected with the various states in Li_4 clusters. As expected, the singlet planar configuration shows occupation of the p_x orbitals only while the triplet shows occupation of both p_x and p_y orbitals. In either case, the p_z states are empty. However, when Li_4 is forced to be three dimensional in structure (tetrahedral in the bcc phase) the occupation of p_z is clearly observed.

D. Magnetism versus cluster geometry

It is now appropriate to discuss the magnetic behavior of small clusters and its relationship to cluster topology. For $N=2$ and $N=3$ clusters the spin configurations are $\uparrow\downarrow$ and $\uparrow\downarrow\uparrow$. Flexibility in these assignments begins to arise with the $N=4$ cluster where we can have either a singlet ($\uparrow\downarrow\uparrow\downarrow$) or a triplet ($\uparrow\downarrow\uparrow\uparrow$) state. For each of these assignments, the geometries have to be optimized. We

TABLE V. Orbital charges associated with a lithium atom in different configurations of Li_4 clusters.

	Configuration			
	Planar		bcc	
Orbital	Singlet	Triplet	Singlet	Triplet
$1s$	1.9887	1.9904	1.9880	1.9899
$2s$	0.5038	0.7671	0.3902	0.6715
$2p_x$	0.3890	0.1437	0.0236	0.0446
$2p_z$	0.0	0.0	0.0620	0.1189
$2p_y$	0.0450	0.1493	0.4299	0.1751

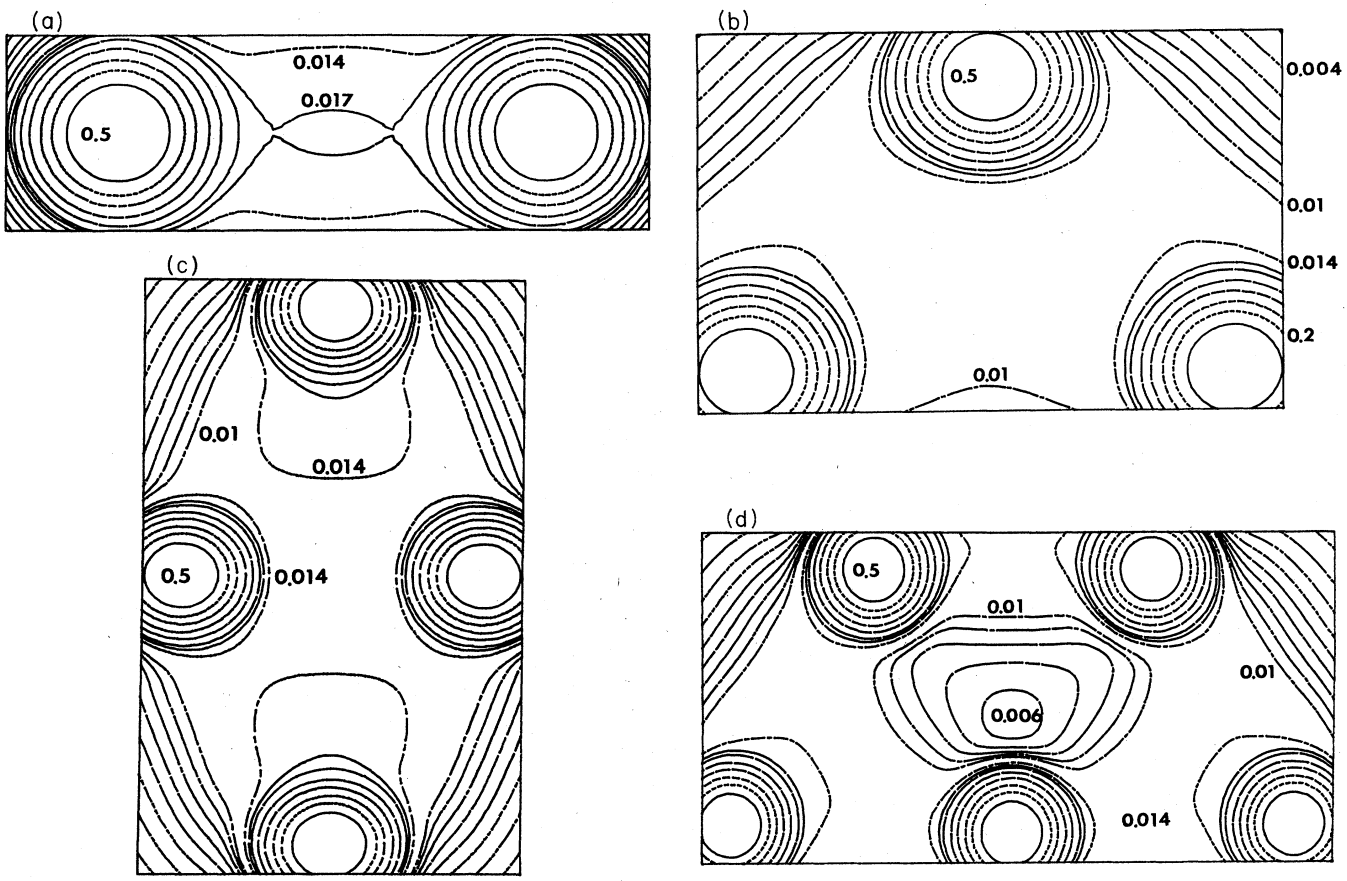

FIG. 4. (a) Charge density contour for Li_2. Starting from the nuclei and moving outward, the charge densities have been given for 0.5, 0.2, 0.1, 0.05, 0.03, 0.02, 0.017, 0.014, 0.01, 0.009, 0.008, 0.007, 0.006, 0.005, and 0.004 a_0^{-3}, respectively. (b) Charge density contour for Li_3. See caption of (a) for details. (c) Charge density contour for Li_4. See caption of (a) for details. (d) Charge density contour for Li_5. See caption of (a) for details.

have actually compared (see Table VI) the total energies for the singlet and triplet states of the $N=4$ cluster in the optimized planar structure. As pointed out earlier, we do see that the $N=4$ cluster prefers to be in a singlet spin state. This is, again, a reconfirmation of our earlier statement that p_x-like, p_y-like, and p_x-like states are filled in succession.

In the discussion of the spin-polarized-jellium calculations, we pointed out that maximizing spins according to Hund's rule always lowers the total energy of the cluster. Thus, in the jellium model, a Li_4 cluster will be magnetic. This result is in contradiction with our calculations on the real cluster. To understand the origin of this discrepancy, we note that the four-atom jellium cluster is three dimensional, whereas the equilibrium geometry is completely planar. To see if the preferred spin orientation is linked to the dimensionality of the cluster, we forced the four Li atoms to have a tetrahedral configuration in the bcc structure. We, then, varied the lattice constant of this cluster for both singlet and triplet spin configurations until the minimum in the energy was achieved. The corresponding total energies and bond lengths for both of these tetrahedral clusters are shown in Table VI along with the planar structures.[34] Note that, in this case, the triplet state has lower energy than the singlet state in agreement with the jellium result. The preferred spin orientation and its relationship with the dimensionality of the cluster can be understood in the following way. An analysis of the populations of the molecular orbitals of the planar clusters reveals that the p_x-, p_y-, and p_z-like states are filled in succession. For the $N=4$ cluster, p_y- and p_z-like states are empty. For the three-dimensional tetrahedral cluster, on the other hand, p_x-, p_y-, and p_z-like states are filled simultaneously, and hence energy can be lowered by max-

TABLE VI. Comparison of energies and bond lengths of Li_4 clusters in optimized planar and bcc (tetrahedral) structures. All calculations are with STO-6G basis and full CI.

Geometry	Quantity	Singlet	Triplet
Planar	Energy	−29.708 516	−29.687 650
	a	2.938	2.848
	b	2.612	3.276
bcc	Energy	−29.674 681	−29.689 877
	Lattice constant	3.246	3.210

imizing spin due to the exchange interaction. In addition, we want to point out that the spin-singlet $N=4$ planar cluster is more compact that the spin-triplet $N=4$ tetrahedral cluster. This leads to a larger electron density along the bond in the two-dimensional cluster as compared to the corresponding three-dimensional one. The increased electron density favors antisymmetry in the spin, making the planar cluster less magnetic. Since the dimensionality of the cluster topology is linked to the magnetic order for $N<7$ in monovalent metals, we can say that the jellium model would predict the wrong spin configuration for $N=4$, 5, 6 clusters. We have found that the equilibrium geometry for $N=5$ in Fig. 2(iv) has the spin orientation $\uparrow\downarrow\uparrow\downarrow\uparrow$ instead of $\uparrow\downarrow\uparrow\uparrow\uparrow$.

IV. CONCLUSIONS

We have performed self-consistent molecular cluster calculations of total energies and electronic properties of Li clusters consisting of $N=1$ to $N=5$ atoms per cluster. Our results can be summarized in the following steps.

(i) We have investigated in detail the dependence of binding energy and bond length of the Li_2 dimer and energy and ionization potential of the Li atom on the choice of basis set. The results are quite sensitive to the basis set used. The basis set which gives the best atomic properties may not necessarily predict the molecular properties with similar accuracy. It is argued that for an understanding of cluster properties, the valence-electron-orbital representation has to be improved. We find that for cluster calculations a basis set should be chosen which can predict the binding energy and bond length of the dimer with most accuracy. The effect of correlation has been investigated by including it perturbatively through pair excitations of valence electrons and all electrons separately as well as through configuration interaction of all pair excitations. While the bond length of the Li_2 dimer is not very sensitive to the level of correlation approximation, the binding energy is strongly influenced by correlation. Using the STO-6G basis, our CI calculation predicts bond length and binding energy of Li_2 in *quantitative* agreement with experiment.

(ii) We have obtained optimized geometries of $N=2$— to $N=5$—atom Li clusters by varying all possible topological parameters until the total energy reached a minimum. All the geometries were found to be planar. In agreement with the observations in Na clusters,[5] we find the clusters of Li form a close-packed structure.

(iii) The effect of correlation did not have much influence either on the equilibrium geometry or on topological parameters. However, the agreement of the dissociation energy with experiment improves considerably when correlation is included.

(iv) The equilibrium geometries of ionized clusters have been obtained in a way similar to that used for neutral clusters. The ionized clusters are found to be more open structures than their corresponding neutral counterparts.

(v) The energy per atom, dissociation energy, and ionization potential have been obtained as a function of the number of atoms in the cluster from both UHF and CI calculations. While the UHF procedure yields optimized geometries and bond lengths in good agreement with CI calculations, the structure in the energy per atom, dissociation energy, and ionization potential are only evident when correlation is taken into account. It is pointed out that simultaneous understanding of all these properties is needed to explain the origin of the magic numbers in the mass spectra. The first two quantities are responsible for the formation and stability of clusters, whereas the third quantity signals the probability of finding abundances in the ionized clusters. In addition to these static properties, dynamic effects may also be important[26] in the study of magic numbers. For transition-metal-atom clusters, core electrons may also play a significant role in the equilibrium geometry and electronic interactions. Thus, the occurrence of magic numbers cannot be regarded as simply arising from the electronic shell structure as implied by recent jellium calculations.[3] Further work is necessary on this point.

(vi) We have found that small clusters can be magnetic. For planar clusters, the preferred spin configuration is different from that expected from Hund's-rule coupling. Hund's rule does not hold true until the cluster assumes a three-dimensional geometry.

(vii) All the arguments presented here are expected to hold true for small clusters of simple metals. For clusters of transition-metal atoms where core electrons are important, the physics may be different. Thus, transition-metal-atom clusters provide an attractive system to study interesting problems in physics and chemistry of molecules. Such an investigation is presently under way.

ACKNOWLEDGMENTS

This work was supported in part by the Thomas F. Jeffress and Kate Miller Jeffress Trust and the National Science Foundation. We are thankful to Dr. Matti Manninen for many helpful discussions and for providing Fig. 2. Many useful comments made by Dr. Shiv Khanna are also appreciated.

*Permanent Address: Institute of Physics, Bhubaneswar 751005, India.

[1]B. Lindgren and D. E. Ellis, Phys. Rev. B **26**, 636 (1982); R. P. Messmer, Surf. Sci. **106**, 225 (1981); A. B. Kunz, in *Theory of Chemisorption,* edited by J. R. Smith (Springer, New York, 1980).

[2]B. K. Rao, P. Jena, and D. D. Shillady, Phys. Rev. B **30**, 7293 (1984).

[3]W. D. Knight, K. Clemenger, W. A. deHeer, W. A. Saunders, M. Y. Chou, and M. L. Cohen, Phys. Rev. Lett. **52**, 2141 (1984).

[4]A. Hintermann and M. Manninen, Phys. Rev. B **27**, 7262 (1983); V. N. Bogorrolov, A. I. Zadorozhnii, L. K. Panina, and V. P. Petranovskii, Zh. Eksp. Teor. Fiz. Pis'ma Red **31**, 371 (1980); [JETP Lett. **31**, 339 (1980)].

[5]J. L. Martins, J. Buttet, and R. Car, Phys. Rev. Lett. **53**, 655

(1984).
[6]W. J. Hehre, R. F. Stewart, and J. A. Pople, J. Chem. Phys. **51**, 2657 (1969).
[7]B. T. Pickup, Proc. R. Soc. London, Ser. A **333**, 69 (1973); R. P. Messmer, Surf. Sci. **106**, 225 (1981); R. F. Marshall, R. J. Blint, and A. B. Kunz, Phys. Rev. B **13**, 3333 (1976); T. H. Upton and W. A. Goddard III, Phys. Rev. Lett. **42**, 472 (1979); J. L. Martins, R. Car, and J. Buttet, J. Chem. Phys. **78**, 5646 (1983); D. W. Davies and G. del Conde, Chem. Phys. **12**, 45 (1976).
[8]P. Fantucci, J. Koutecký, and G. Pacchioni, J. Chem. Phys. **80**, 325 (1984).
[9]W. H. Gerber and E. Schumacher, J. Chem. Phys. **69**, 1692 (1978).
[10]J. L. Cole, R. H. Childs, D. A. Dixon, and R. A. Eades, J. Chem. Phys. **72**, 6368 (1980); G. Pacchioni, H.-O. Beckmann, and J. Koutecký, Chem. Phys. Lett. **87**, 151 (1982).
[11]T. B. Grimley, J. Phys. B **16**, 1125 (1983).
[12]J. A. Pople and R. K. Nesbet, J. Chem. Phys. **22**, 571 (1954).
[13]W. J. Hehre, R. Ditchfield, R. F. Stewart, and J. A. Pople, J. Chem. Phys. **52**, 2769 (1970).
[14]R. Ditchfield, W. J. Hehre, and J. A. Pople, J. Chem. Phys. **54**, 724 (1971).
[15]W. J. Hehre, R. Ditchfield, and J. A. Pople, J. Chem. Phys. **56**, 2257 (1972).
[16]A. Johansson, P. Kollman, and S. Rottenberg, Theor. Chim. Acta **19**, 167 (1973); S. L. Price and A. J. Stone, Chem. Phys. Lett. **65**, 127 (1979).
[17]C. Møller and M. S. Plesset, Phys. Rev. **46**, 618 (1934).
[18]J. S. Binkley and J. A. Pople, Int. J. Quant. Chem. **9**, 229 (1975).
[19]J. S. Binkley and J. A. Pople, J. Chem. Phys. **66**, 879 (1977).
[20]T. H. Dunning, J. Chem. Phys. **55**, 716 (1971).
[21]To the basis sets of Ref. 20, two p functions were added with optimized scale factors and then contracted.
[22]See, for example, S. Huzinaga and Y. Sakai, J. Chem. Phys. **50**, 1371 (1969).
[23]A. Hermann, E. Schumacher, and L. Wöste, J. Chem. Phys. **68**, 2317 (1978); M. M. Kappes, R. W. Kunz, and E. Schumacher, Chem. Phys. Lett. **91**, 413 (1982).
[24]K. Kimoto, I. Nishida, H. Takahashi, and H. Kato, Jpn. J. Appl. Phys. **19**, 1821 (1980).
[25]O. Echt, K. Sattler, and E. Recknagel, Phys. Rev. Lett. **47**, 1121 (1981); A. Ding and J. Hesslich, Chem. Phys. Lett. **94**, 54 (1983); P. W. Stephens, and J. G. King, Phys. Rev. Lett. **51**, 1538 (1983).
[26]M. Manninen (unpublished).
[27]P. Hohenberg and W. Kohn, Phys. Rev. **136**, B964 (1964); W. Kohn and L. J. Sham, *ibid.* **140**, A1133 (1965); A. K. Rajagopol and J. Callaway, Phys. Rev. B **7**, 1912 (1973).
[28]B. K. Rao, P. Jena, and M. Manninen, Phys. Rev. B (to be published).
[29]B. K. Rao and P. Jena (unpublished).
[30]K. P. Huber and G. Herzberg, *Molecular Spectra and Molecular Structure,* Vol. 4 of *Constants of Diatomic Molecules* (Van Nostrand, New York, 1979).
[31]G. Das, J. Chem. Phys. **46**, 1568 (1967).
[32]C. H. Wu, J. Chem. Phys. **65**, 3181 (1976).
[33]C. H. Wu, J. Phys. Chem. **87**, 1534 (1984).
[34]These are in agreement with the recent results of D. Plavcic, J. Phys. Chem. **87**, 1096 (1984).